

## RESEARCH ARTICLE

# Is a passivated back contact always beneficial for Cu (In,Ga)Se<sub>2</sub> solar cells?

Ye Tu<sup>1</sup> | Yong Li<sup>2</sup> | Reiner Klenk<sup>3</sup> | Guanchao Yin<sup>1</sup>  | Martina Schmid<sup>2</sup>

<sup>1</sup>School of Materials Science and Engineering, Wuhan University of Technology, Wuhan, China

<sup>2</sup>Faculty of Physics, University of Duisburg-Essen and CENIDE, Duisburg, Germany

<sup>3</sup>PVComB/Helmholtz-Zentrum Berlin für Materialien und Energie, Berlin, Germany

## Correspondence

Guanchao Yin, School of Materials Science and Engineering, Wuhan University of Technology, Luoshi Road 122, Wuhan 430070, China.  
Email: guanchao.yin@whut.edu.cn

## Abstract

Ultrathin CIGSe solar cells on TCOs (transparent conductive oxides) have many promising potential applications due to their transparency. However, their performance is strongly constrained due to the back contact, often referred to acting as a Schottky junction. In this work, we show that the current limitation due to a back Schottky junction can be responsible for the apparent photocurrent loss and suppression of the forward current, which deteriorates cell performance and leads to the S-shaped *J*-*V* characteristics, respectively. However, due to the non-negligible photocurrent in the back Schottky diode and the current amplification effect of a transistor, cells with a reduced absorber thickness overall exhibit a relieved current suppression, resulting in a light *J*-*V* curve closer to the one with an Ohmic back contact. Notably, a higher back interface recombination velocity is capable of increasing the forward current of the Schottky diode by recombination, which mitigates the limitation of current flow through the back Schottky junction and thus improves the cell performance. The results show strong implications that introducing high density defects at the back interface is favorable for CIGSe solar cells on TCOs, rather than employing point-contact structures for interface passivation. This suggests a different path to improve ultrathin CIGSe solar cells on TCOs compared to the devices on Mo with an Ohmic back contact.

## KEYWORDS

back recombination, CIGSe solar cells, hole transport, point contact, Schottky contact

## 1 | INTRODUCTION

Compared to conventional ones with an absorber thickness beyond 2 μm, ultrathin Cu (In,Ga)Se<sub>2</sub> (CIGSe) solar cells (with a sub-500 nm absorber) hold the unique advantage to reduce the material consumption.<sup>1–3</sup> This allows to largely relax concerns of indium scarcity and lower the material-related cost in mass production, which can potentially improve the competitiveness of CIGSe solar cells in the photovoltaic market.<sup>4,5</sup> However, their efficiencies are up to now not competitive, and insufficient absorption and back recombination mainly account for the poor performance.<sup>1–3,6,7</sup>

Back recombination is the loss of photogenerated electrons transporting to the back interface (Mo/CIGSe) and recombining

there.<sup>1,2,6,7</sup> Since the back contact is within the diffusion length of photogenerated minorities (electrons here), back recombination is extraordinarily severe for ultrathin CIGSe solar cells. In the last few years, point-contact nanostructures made of dielectric materials, which were adapted from Si technology, were emerging to passivate the back interface, and thus reduce back recombination for ultrathin CIGSe solar cells.<sup>8–18</sup> This is arising from the presence of a high density of negative internal charges as well as a low density of interface defects on the point-contact nanostructures, overall giving rising to a lower surface recombination at the back interface.<sup>8,9,12,13</sup> Simultaneously, dielectric point-contact nanostructures can enhance the optical reflectivity of Mo/CIGSe and significantly improve light absorption.<sup>9–17</sup> In combination, both electrical and optical effects

yield a pronounced performance enhancement for ultrathin CIGSe solar cells on Mo.

Besides on Mo, CIGSe solar cells can alternatively be prepared on transparent conductive oxides (TCOs).<sup>19–22</sup> Compared to the optically lossy Mo, their transparency renders many unique advantages. For instance, TCO substrates favor the realization of pronounced light trapping in ultrathin CIGSe solar cells.<sup>23–27</sup> Furthermore, CIGSe solar cells on TCOs can be utilized in tandem cells as a top cell,<sup>28</sup> bifacial solar cells,<sup>29,30</sup> in solar window, and in backwall configuration.<sup>31,32</sup> It should be noted that, due to the high temperature during CIGSe absorber deposition, TCOs may be thermally unstable<sup>19,20</sup> and ITO (Sn: In<sub>2</sub>O<sub>3</sub>) and FTO (F:SnO<sub>2</sub>) are experimentally preferred.<sup>19,21,22</sup> Compared to cells on Mo with an Ohmic back contact, CIGSe solar cells on *n*-TCOs, due to the mismatch of conductivity type, typically exhibit a back barrier potential and thus a space charge region opposed to the main *pn* junction, hence acting similarly to a Schottky diode.<sup>20,32–35</sup> This will typically lead to an S-shaped light *J*-*V* curve (rollover effect) and a crossover between light and dark *J*-*V* curves.<sup>36,37</sup> On the other hand, some authors did not observe those non-ideal characteristics and claimed that the TCO/CIGSe back contact is quasi-Ohmic.<sup>19,22,36,38</sup> Recently, several publications reported that an increased back recombination is likely to lessen the impact of the back barrier potential for cells on ITO and to improve the cell performance.<sup>22,36,39</sup> This may pose a sharp contrast to previous demonstrations for cells on Mo, where a reduced back recombination is desirable. Up to now, the relevant explorations of passivating back contacts have mainly been confined to cells on Mo with an Ohmic contact.<sup>8–18</sup> Since cells on TCOs may exhibit a Schottky-like back contact with a barrier potential, this may bring a different carrier transport behavior from the condition with an Ohmic contact. Further, considering promising applications and relatively poor performance of ultrathin CIGSe solar cells on TCOs, it will be of great interest to identify how a passivated back contact affects CIGSe solar cells with a Schottky back contact. Strictly speaking, a Schottky diode can be merely formed between a metal and a semiconductor, whereas the junction at the back interface is *n*<sup>+</sup>*p* for CIGSe solar cells on TCOs. In fact, several authors have not made that distinction and claim that a Schottky back contact forms between CIGSe and TCOs.<sup>33–35</sup> However, in both cases, there is a band bending only in the absorber near the back contact and thus effects on the carrier transport are quite similar. Therefore, we here assume that a Schottky diode can be used for modeling the TCO/CIGSe junction.

In this work, we employ the one-dimensional modeling software SCAPS<sup>40</sup> and theoretically investigate how a passivated back contact affects solar cells with a Schottky back contact. It is demonstrated that, compared to cells with an Ohmic contact, it is the current limitation introduced by the back Schottky diode, which is responsible for the relatively poor cell performance and the forward current suppression. Cells with a reduced absorber thickness show a less severe current suppression compared to their thick counterparts, as a joint result of the non-negligible photocurrent in the back Schottky diode and the amplification effect of a transistor. Increasing the back interface recombination velocity is able to increase the forward current of

the back Schottky diode by assisting hole recombination, which thereby alleviates the current limitation by the back Schottky junction and improves the cell performance. It strongly implies that introducing a high density of defect states at the back contact is favorable to the performance of ultrathin CIGSe cells on TCOs. This poses a striking contrast to CIGSe cells on Mo (Ohmic contact), where employing point-contact structures and passivating back contacts is desirable.

## 2 | SIMULATION MODEL

The one-dimensional software SCAPS<sup>40</sup> is applied for all simulations, which is developed specially for CIGSe and CdTe solar cells. For a clear identification of the effect of the back Schottky junction on the cells and to avoid any interference of band discontinuities in the heterojunction cell, we take a simple homojunction cell structure with constant band gap in our model. As illustrated in Figure 1, the cell is composed of Layer 1 (200 nm, illumination side)/Layer 2 (*d* nm)/Layer 3 (20 nm)/back contact from top to bottom, without band discontinuities or defects at the interfaces between Layer 1/Layer 2/Layer 3. The three layers have the same parameters except for layer thickness and doping type. Layer 1 is *n* type, and the other two are *p* type. The *pn* junction is hence formed at the interface between Layers 1 and 2. All three layers have a band gap of 1.2 eV, and a moderate doping concentration of 1E16 cm<sup>−3</sup> is assumed. A mid-gap neutral defect is introduced in each layer, which sets a lifetime of 100 ns and a diffusion length of 1.1 μm for both electrons and holes. Since the ultimate goal in this contribution is to identify how the back barrier potential affects CIGSe cells, relevant parameters related to absorber and back contact are chosen such that they are realistic for CIGSe solar cells.<sup>41–43</sup> This implies that, despite the modeled cell structure deviating from the real cells to some extent, the main conclusions will not be affected by this simplification.

To investigate the effects of back recombination for cells with a Schottky back contact, the back recombination velocities *S*<sub>b</sub> for electrons and holes are assumed the same and range from 1E2 to 1E6 cm/s. The back potential *E*<sub>b</sub> (barrier height for majority carriers, with respect to the equilibrium valence band) is set to 0.4 eV. All relevant parameters are summarized in Table 1, and a sketch of the resulting band diagram is shown in Figure 1. The definition file can be obtained directly from the authors.

## 3 | RESULTS AND DISCUSSION

### 3.1 | Thick cells

We start from a thick Layer 2 (*d* = 2,000 nm), which keeps the back contact away from the main *pn* junction formed by Layer 1/Layer 2. Figure 2 shows light *J*-*V* curves for various conditions at a fixed interface recombination velocity *S*<sub>b</sub> of 1E2 cm/s. Compared to the condition with an Ohmic back contact (black solid line), a Schottky contact (*E*<sub>b</sub> = 0.4 eV here) indeed generates the S-shaped characteristic

**FIGURE 1** Sketch of the band diagram of the investigated solar cell structure with back potential  $E_h = 0.4$  eV and recombination velocity  $S_b = 1\text{E}6$  cm/s at zero bias.  $E_c$  and  $E_v$  are the conduction and valence band edges, respectively;  $F_n$  and  $F_p$  are the quasi Fermi levels of electrons and holes, respectively

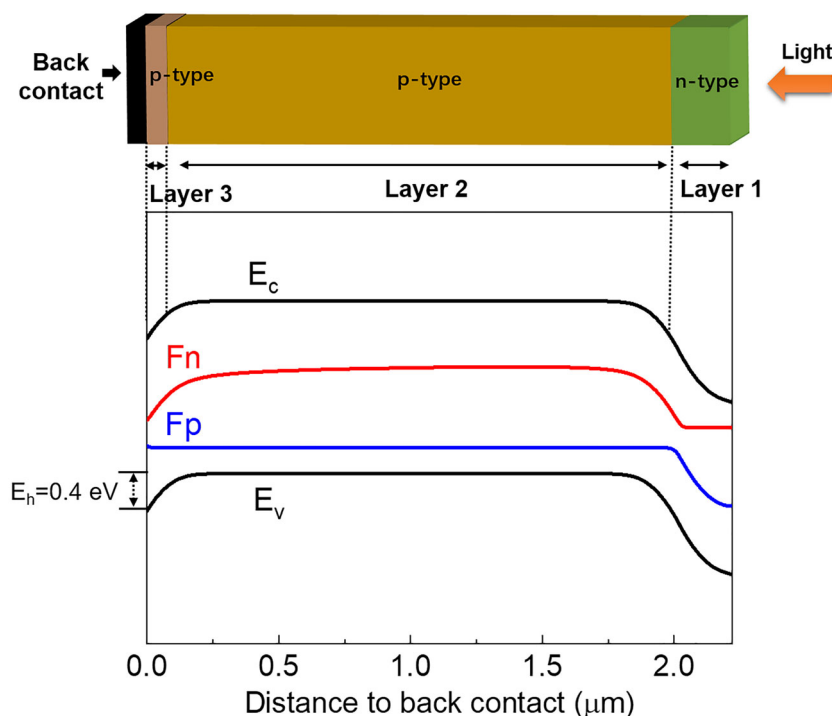


**TABLE 1** Device parameters of a simplified solar cell structure for simulations

Layer properties	Back contact	Layer 3	Layer 2	Layer 1
$d$ (nm)	x	20	$d$ (variable)	200
$E_g$ (eV)	x	1.2	1.2	1.2
$\chi$ (eV)	x	4.5	4.5	4.5
$\epsilon/\epsilon_0$	x	10	10	10
$N_C$ (cm $^{-3}$ )	x	1.0E19	1.0E19	1.0E19
$N_V$ (cm $^{-3}$ )	x	1.0E19	1.0E19	1.0E19
$\mu_n$ (cm $^2$ V $^{-1}$ s $^{-1}$ )	x	50	50	50
$\mu_p$ (cm $^2$ V $^{-1}$ s $^{-1}$ )	x	50	50	50
$\tau_n$ (ns)	x	100	100	100
$\tau_p$ (ns)	x	100	100	100
$L_n$ (μm)	x	1.1	1.1	1.1
$L_p$ (μm)	x	1.1	1.1	1.1
$\nu_{th}$ (cm s $^{-1}$ )	x	1.0E7	1.0E7	1.0E7
$N_{D/A}$ (cm $^{-3}$ )	x	1.0E16	1.0E16	1.0E16
$S_b$ (cm/s)	variable	x	x	x
$E_h$ (eV)	0.4	x	x	x

Abbreviations:  $d$ , thickness of layer 2;  $E_g$ , bandgap;  $E_h$ , back potential barrier with respect to valence band;  $L_{n/p}$ , electron/hole diffusion length;  $N_{C/V}$ , density of states in conduction/valence band;  $N_{D/A}$ , effective donor/acceptor doping;  $S_b$ , interface recombination velocity at CIGSe/back contact;  $\epsilon/\epsilon_0$ , relative permeability;  $\mu_{n/p}$ , electron/hole mobility;  $\tau_{n/p}$ , electron/hole bulk lifetime;  $\nu_{th}$ , thermal velocity;  $\chi$ , electron affinity.

(red solid line) and deteriorates the cell performance mainly by a lower  $V_{oc}$  (open-circuit voltage) and  $FF$  (fill factor), which agrees well with previous results.<sup>20,30–35</sup> Since the Schottky back contact generates a potential barrier for holes passing towards the back contact, it has been claimed previously that the back barrier blocks the transport of photogenerated holes and thereby deteriorates the cell

performance.<sup>32,35</sup> If this were true, a CIGSe absorber layer close to the back contact with a valence band offset should produce a similar blocking effect. To test it, we set Layer 3 (close to the back contact, 20 nm thick) to produce a valence band offset of 0.4 eV by increasing its bandgap by 0.4 eV at a fixed electron affinity. The corresponding  $J$ - $V$  curve (green dashed line) is also included in Figure 2. Notably,

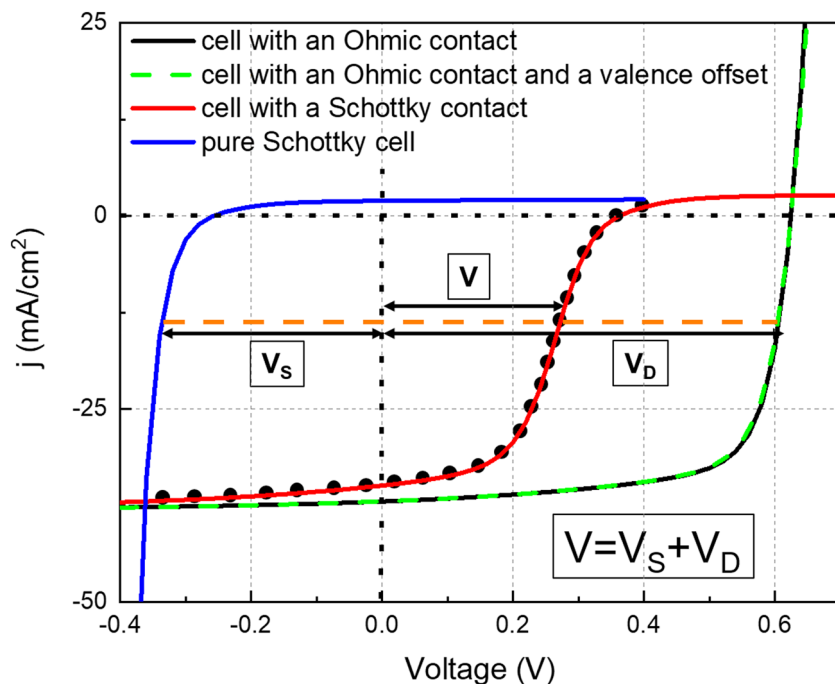


**FIGURE 2** Light  $J$ - $V$  curves for various back configurations at  $S_0$  of  $1\text{E}2\text{ cm/s}$  (Layer 2: thickness  $d = 2,000\text{ nm}$ )

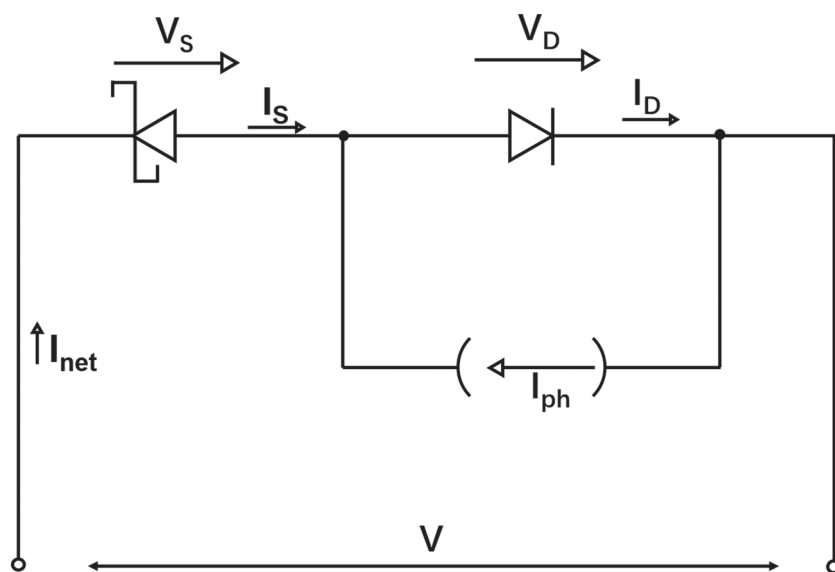


**FIGURE 3** Equivalent circuit of a solar cell with a reverse Schottky diode at the back contact

compared to the pure Ohmic-contact cell, the additional valence band offset hardly changes the light  $J$ - $V$  curve. Actually, it is the photogenerated minorities (electrons here) which determine the photocurrent,<sup>41</sup> indicating that the modification in the valence band exerts only a marginal effect on the photocurrent. Therefore, the blocking of photogenerated holes is not the critical factor for a Schottky back contact which is harming the cell performance.

To identify how the Schottky back contact really affects the cell performance, the  $J$ - $V$  curve of the pure back Schottky cell (blue solid line) is calculated by switching the conductivity type of Layer 1 ( $n$  to  $p$ ) and included in Figure 2 as well. Since the polarity of the Schottky junction is opposite to the  $pn$  junction between Layer 1/Layer 2, its forward bias is pointing to the negative  $x$  direction and its forward

current to the negative  $y$  direction. The Schottky cell has a small photocurrent and starts to exhibit a net forward current at a bias of  $-0.25\text{ V}$  (corresponding to its  $V_{oc}$ ). We interpolate the  $J$ - $V$  curves of the cell with a pure Ohmic contact (black solid line) and the pure Schottky cell (blue solid line) and add the corresponding voltages at equal currents. As the solid circles indicate, the voltage addition is equal to the simulated value for the cell with the Schottky back contact (red solid line). This finding reflects that the two diodes, that is, the  $pn$  junction and the Schottky diode, are in series connection in the equivalent circuit, which is sketched in a simplified version without considering shunt and series resistances in Figure 3.

From the sketch, we see that the current  $I_S$  through the Schottky junction equals the net current  $I_{net}$  of the circuit and obeys:

$$I_{\text{net}} = I_S = I_D - I_{\text{ph}}, \quad (1)$$

where  $I_D$  is the diode current through the  $pn$  junction and  $I_{\text{ph}}$  the photocurrent.

Besides,  $I_S$  follows the following equation<sup>44</sup>:

$$I_S = -I_{S0}(\exp(-qV_S/kT) - 1), \quad (2)$$

where  $I_{S0}$  is the saturation current,  $q$  the elementary charge,  $k$  the Boltzmann constant, and  $T$  the Kelvin temperature. The minus signs in front of  $I_{S0}$  and  $V_S$  indicate the opposite polarity of the Schottky diode with respect to the  $pn$  junction.

The voltage  $V$  across the whole circuit is the sum of  $V_S$  and  $V_D$  as Equation 3 shows. Since  $V_S$  and  $V_D$  are functions of their individual passing currents, the voltage across the whole circuit is denoted as

$$V = V_S(I_D - I_{\text{ph}}) + V_D(I_D). \quad (3)$$

In the fourth quadrant, as the orange dashed line in Figure 2 exemplarily shows for a fixed current, the current through the Schottky diode  $I_S$  (or the net current  $I_{\text{net}}$ ) is in the same direction as the photocurrent  $I_{\text{ph}}$ , pointing towards the back contact. Due to the Schottky junction being a majority device, the forward dark current here are holes being transported towards back contact. This means that the Schottky junction is under the condition of a forward bias and  $V_S$  is thus in an opposite direction to the bias across the  $pn$  junction  $V_D$ . Consequently, according to Equation 3,  $V_D$  across the  $pn$  junction will be higher than the applied voltage  $V$  across the whole circuit (which is also reflected in Figure 2). This will in turn lead to a larger  $I_D$  and thus reduces  $I_S$  (or  $I_{\text{net}}$ ) based on Equation 1. It shall be stressed that (as shown in Equation 2) the current  $I_S$  is exponentially depending on the applied bias  $V_S$  for a Schottky diode, whereas for the condition of an Ohmic contact,  $V_D$  simply equals the bias across the whole circuit  $V$  and  $I_{\text{net}}$  is not limited by the current through the back Schottky diode  $I_S$ . Therefore, we conclude that the apparent loss in photocurrent in the fourth quadrant is due to the restraint of current introduced by the back Schottky diode.

In the first quadrant in Figure 2,  $I_D$  is larger than  $I_{\text{ph}}$ , leading to the net current  $I_{\text{net}}$  (or  $I_S$ ) transporting in the opposite direction to  $I_{\text{ph}}$ . According to the Schottky diode equation (Equation 2),  $I_{\text{net}}$  or  $I_S$  will be heavily limited by  $I_{S0}$ , which is barely bias-dependent for a Schottky diode. This determines that the net forward current is suppressed in the first quadrant for the cell with a Schottky back contact. Unlike a pure resistor, the Schottky junction exhibits a photocurrent (though it is small here and has been neglected in the equivalent circuit for a thick absorber in Figure 3), and  $V_S$  takes a negative value rather than being zero at short-circuit condition ( $I_S = 0$ ). According to the addition principle of voltages ( $V = V_S + V_D$ ) stated above, it can be inferred that a back Schottky diode deteriorates  $V_{\text{oc}}$  as well, whereas a pure resistor will not.

Figure 4A plots light  $J$ - $V$  curves for the solar cell with a Schottky back contact at various interface recombination velocities ( $S_b = 1\text{E}2$ - $1\text{E}6$  cm/s). Notably, a higher  $S_b$  points to a reduced

photocurrent loss, leading to an optimum  $FF$  and  $V_{\text{oc}}$  obtained at the highest  $S_b$  of  $1\text{E}6$  cm/s. Since the  $pn$  junction and the Schottky junction are in series connection as concluded above and  $S_b$  has a marginal effect on thick cells with an Ohmic contact,<sup>8</sup> the effect of  $S_b$  on the cell with a Schottky contact actually lies in how  $S_b$  affects the  $J$ - $V$  evolution of the pure Schottky cell. Figure 4B represents light  $J$ - $V$  curves of the pure Schottky cell at various  $S_b$ . At a lower  $S_b$ , the forward current (in negative  $x$  direction) is more limited. Conversely, a higher  $S_b$  corresponds to a larger forward diode current and thus relaxes the current limitation introduced by the back Schottky diode. It hence alleviates the deterioration of  $V_{\text{oc}}$  and  $FF$ . As stated above, the Schottky cell is a majority device, and the forward dark current is holes going towards the back contact. The dependence of forward current on  $S_b$  implies that a higher  $S_b$  is capable of assisting holes going through the back interface. As Figure 4C illustrates, the back contact has a relatively low work function and is thus not selective to holes. This determines that the forward hole current from the p-typed semiconductor to back contact is likely to be realized in terms of recombination.

### 3.2 | Thin solar cells

When the thickness of Layer 2 is reduced to 300 nm, the space charge region (SCR) of the Schottky junction is only around 50 nm away from that of the main  $pn$  junction (estimated from the band diagram). Figure 5A plots light  $J$ - $V$  curves in dependence of  $S_b$  for the cell with a Schottky back contact. A similar trend is observed as shown in Figure 4A: A higher  $S_b$  improves  $V_{\text{oc}}$  and  $FF$ . The remarkable difference is, even at an  $S_b$  of  $1\text{E}2$  cm/s, the current suppression in the first quadrant is not as pronounced as in thick cells. Furthermore, the S-shape characteristic is not visible and  $J$ - $V$  curves resembling those of cells with an Ohmic contact appear as  $S_b$  evolves to  $1\text{E}4$  and  $1\text{E}6$  cm/s. These  $J$ - $V$  curves were also experimentally observed by some authors, and a (quasi-)Ohmic contact was hence claimed to form in CIGSe cells on TCOs.<sup>19,22,36,38</sup> However, the simulations here indicate that this does not necessarily mean that the Schottky diode is absent and an Ohmic back contact is formed. Compared to thick cells, one of the reasons for the mitigation of the S-shaped characteristic is that for thin cells, the corresponding photocurrent in the back Schottky diode is not negligible and points to the direction of the forward current of the main  $pn$  diode.

We also simulated light  $J$ - $V$  curves for the cell with an Ohmic contact and a pure Schottky cell for  $S_b = 1\text{E}2$  cm/s and did the same addition as specified for Figure 2. Interestingly, the added  $J$ - $V$  curve (indicated by the black solid circles) lies to the right side of the directly simulated one for the cell with a Schottky contact when the bias is approaching  $V_{\text{oc}}$  and beyond. It indicates that, compared to their thick counterparts, there are extra effects to relieve the suppression of net forward current for the ultrathin cells with a Schottky back contact. The transistor effect is responsible for it. When the Schottky back contact is approaching the  $pn$  junction, the cell structure can be interpreted as a transistor with a collector, a base and an emitter.<sup>45</sup> The net forward current will be the result of the base current multiplied by

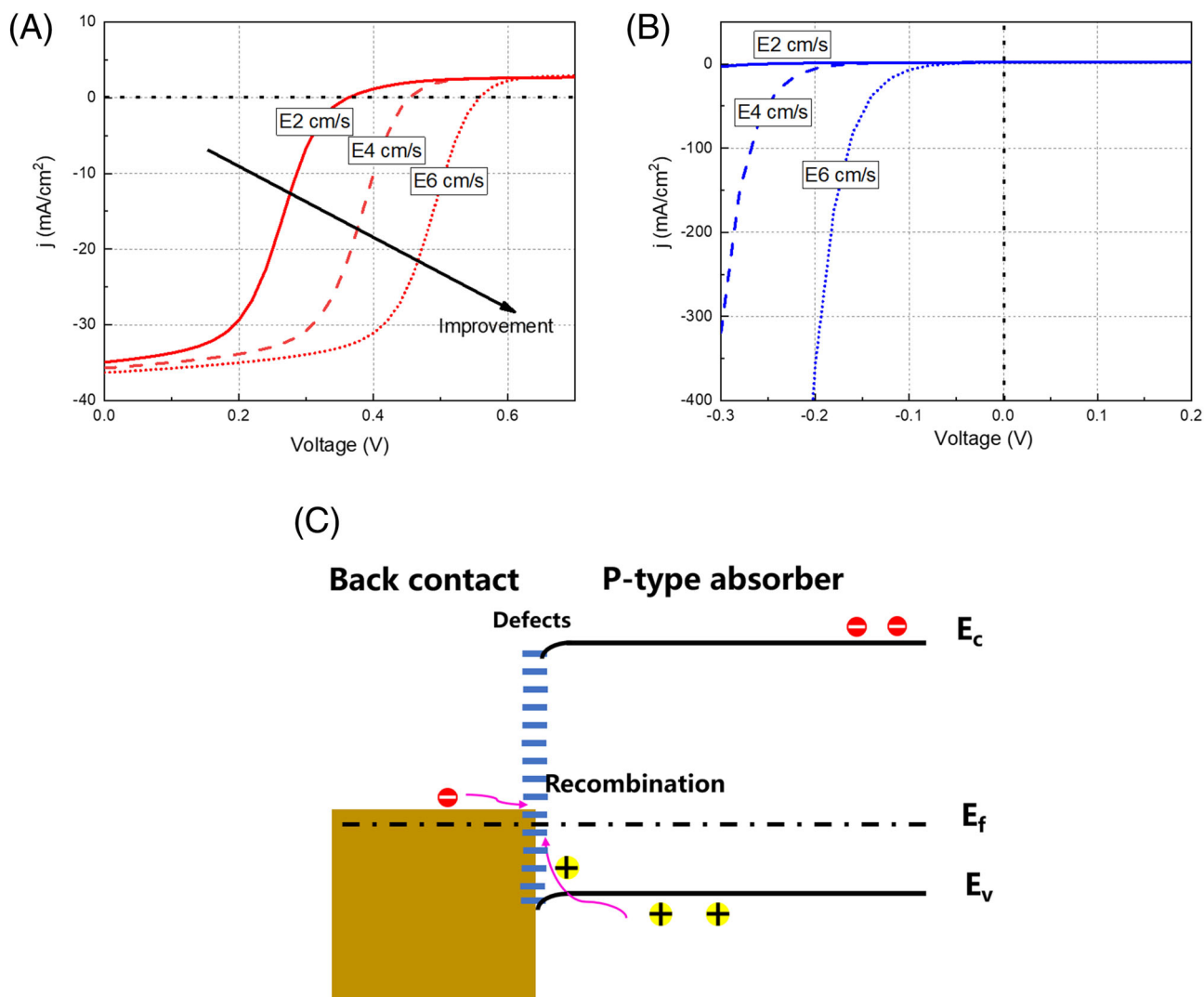


**FIGURE 4** Light J-V curves for (A) a solar cell with a Schottky back contact and (B) the corresponding pure Schottky cell as a function of back interface recombination velocity  $S_b$  (Layer 2: thickness  $d = 2,000$  nm), and (C) sketch of hole transport through the back contact (forward diode current) via defects at the interface

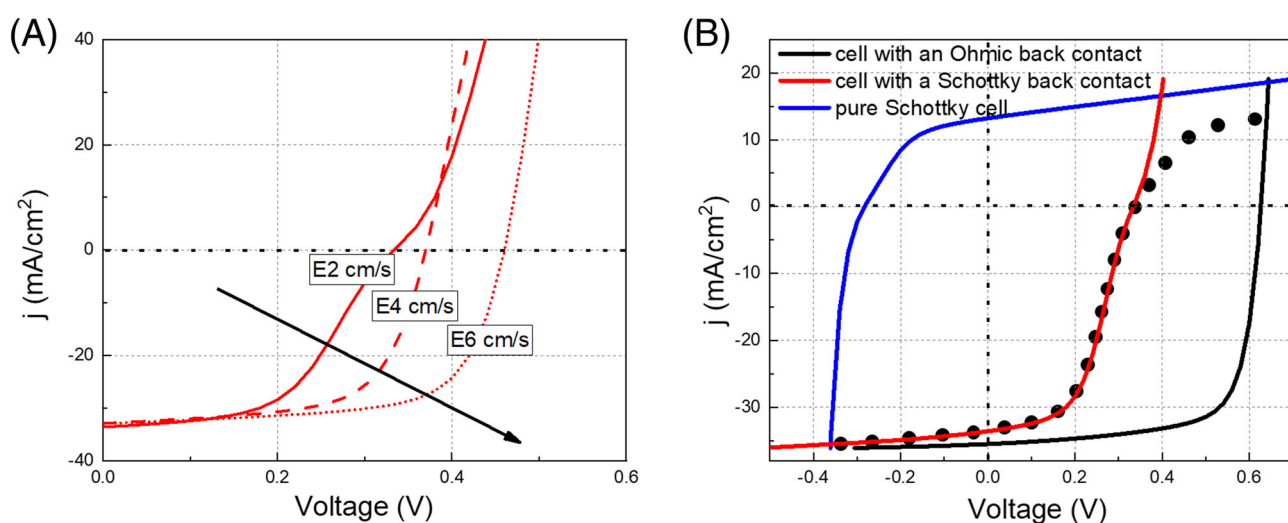


**FIGURE 5** Light J-V curves for (A) a solar cell with a Schottky back contact for varied back recombination velocity  $S_b$  and (B) various back contact configurations at an  $S_b$  of 1E2 cm/s (Layer 2: thickness  $d = 300$  nm)



the amplification  $\beta$  of the transistor, thus leading to a larger current in the simulated  $J$ - $V$  curve (red line) than in the one generated by addition (black solid circle) in the first quadrant.

The critical distance between the back Schottky diode and the front  $pn$  junction, where the transistor effect starts to matter, depends very much on the doping levels of the individual layers. For a realistic CIGSe solar cell, the  $n$ -type window layers have a higher doping level, and the transistor effect can thus be significant at a larger distance between the main  $pn$  junction and the back Schottky diode. This implies that the transistor effect is likely to play a role even in thick realistic CIGSe solar cells with a Schottky back contact.<sup>45</sup>

### 3.3 | Implication for ultrathin CIGSe solar cells on TCOs

To further demonstrate the applicability of the investigated cell structure and related analysis above for realistic CIGSe solar cells, we simulated the dependence of  $S_b$  on light  $J$ - $V$  curves for heterojunction CIGSe cells with a back potential barrier of 0.4 eV (see Supporting Information S1). Similar to what was observed in Figures 4A and 5A, an increasing  $S_b$  mitigates the current limitation and contributes to a continuous improvement in  $FF$  and  $V_{oc}$  for both thick and ultrathin cells. Besides, ultrathin CIGSe solar cells exhibit a less pronounced current suppression in contrast to thick cells. Those results indicate that the simple assumption of a homojunction cell is reasonable enough to explore effects of the back Schottky diode on CIGSe solar cells and interpretations deduced from the simple homojunction model are relevant for realistic CIGSe solar cells.

Introducing point-contact nanostructures for passivating the back contact in ultrathin CIGSe solar cells was intensively explored on Mo, and a significant improvement of electrical properties was validated.<sup>8–18</sup> In contrast to this case of an Ohmic back contact, CIGSe solar cells on TCO substrates are typically treated having a Schottky-like back contact with a back barrier potential. For the latter case, the theoretical study here implies that introducing point-contact structures into ultrathin CIGSe solar cells on TCOs for passivating the back interface, if in the absence of other effects (e.g., electrical field potential<sup>8,12</sup>), is not favorable since the passivated back contact can impair the electrical properties of the cells. Conversely, this study paves a path to improve the performance of ultrathin CIGSe solar cells on TCOs by introducing a high density of defect states at the back interface.

## 4 | CONCLUSION AND OUTLOOK

In this work, we theoretically investigated how a Schottky back contact impacts thin film solar cells. It has been verified that the limitation of the current introduced by the back Schottky diode accounts for the apparent photocurrent loss and the forward current suppression of light  $J$ - $V$  curves. It heavily deteriorates the electrical properties of the solar cells by decreasing both  $FF$  and  $V_{oc}$ .

However, for cells with a reduced absorber thickness, both, the non-negligible photocurrent in the back Schottky diode and the current amplification effect of a transistor, contribute to a large mitigation of the forward current suppression. A higher back interface recombination velocity can alleviate the apparent photocurrent loss, which improves  $FF$  and  $V_{oc}$  simultaneously. This is realized by improving the forward current of the back Schottky diode by assisting hole transport towards the back contact. These findings suggest a different optimization strategy compared to cells with an Ohmic back contact, where passivation of the back contact is desirable. We conclude that implementing point-contact nanostructures to electrically passivate the back interface, which has been successfully employed for performance enhancement of CIGSe solar cells on Mo, may be not applicable for cells on TCOs with a Schottky-like back contact. Conversely, introducing a high density of defects at the back contact is likely to enhance the performance for cells on TCO with a Schottky-like back contact.

### ACKNOWLEDGMENTS

All authors would like to express their sincere gratitude to Marc Burgelman for SCAPS support. Y. Tu and G. Yin acknowledge the funding from National Natural Science Foundation of China (NSFC, 51802240).

### DATA AVAILABILITY STATEMENT

The data that support the findings of this study are available from the corresponding author upon reasonable request.

### ORCID

Guanchao Yin  <https://orcid.org/0000-0002-5545-2595>

### REFERENCES

1. Lundberg O, Bodegård M, Malmström J, Stolt L. Influence of the Cu(In,Ga)Se<sub>2</sub> thickness and Ga grading on solar cell performance. *Prog. Photovolt. Res. Appl.* 2003;11(2):77–88.
2. Gloeckler M, Sites J. Potential of submicrometer thickness Cu(In,Ga)Se<sub>2</sub> solar cells. *J Appl Phys.* 2005;98(10):103703.
3. Bouttemy M, Tran-Van P, Gerard I, et al. Thinning of CIGS solar cells: Part I: Chemical processing in acidic bromine solutions. *Thin Solid Films.* 2011;519(21):7207–7211.
4. Tao CS, Jiang J, Meng T. Natural resource limitations to terawatt-scale solar cells. *Sol. Energy Mater. Sol. Cells.* 2011;95(12):3176–3180.
5. Haegel NM, Margolis R, Buonassisi T, et al. Terawatt-scale photovoltaics: trajectories and challenges. *Science.* 2017;356:141–147.
6. Yin G, Brackmann V, Hoffmann V, Schmid M. Enhanced performance of ultra-thin Cu(In,Ga)Se<sub>2</sub> solar cells deposited at low process temperature. *Sol. Energy Mater. Sol. Cells.* 2015;132:142–147.
7. Mansfield LM, Kanevce A, Harvey SP, et al. Efficiency increased to 15.2% for ultra-thin Cu(In,Ga)Se<sub>2</sub> solar cells. *Prog Photovolt Res Appl.* 2018;26(11):949–954.
8. Vermang B, Fjällström V, Pettersson J, Salomé P, Edoff M. Development of rear surface passivated Cu(In,Ga)Se<sub>2</sub> thin film solar cells with nano-sized local rear point contacts. *Sol Energy Mater sol Cells.* 2013;117:505–511.
9. Vermang B, Wätjen JT, Fjällström V, et al. Employing Si solar cell technology to increase efficiency of ultra-thin Cu(In,Ga)Se<sub>2</sub> solar cells. *Prog. Photovolt. Res. Appl.* 2014;22(10):1023–1029.

10. Casper P, Hünig R, Gomard G, et al. Optoelectrical improvement of ultra-thin Cu(In,Ga)Se<sub>2</sub> solar cells through microstructured MgF<sub>2</sub> and Al<sub>2</sub>O<sub>3</sub> back contact passivation layer. *Phys Status Solidi – Rapid Res Lett*. 2016;10:376-380.
11. Jarzemowski E, Fuhrmann B, Leipner H, Fränzel W, Scheer R. Ultrathin Cu(In,Ga)Se<sub>2</sub> solar cells with point-like back contact in experiment and simulation. *Thin Solid Films*. 2017;633:61-65.
12. Kotipalli R, Poncelet O, Li G, et al. Addressing the impact of rear surface passivation mechanisms on ultra-thin Cu(In,Ga)Se<sub>2</sub> solar cell performances using SCAPS 1-D model. *Sol Energy*. 2017;157:603-613.
13. Salomé PMP, Vermang B, Ribeiro-andrade R, et al. Passivation of interfaces in thin film solar cells: understanding the effects of a nanostructured rear point contact layer. *Adv Mater Interfaces*. 2018;5(2):1701101.
14. Yin G, Song M, Duan S, et al. Well-controlled dielectric nanomeses by colloidal nanosphere lithography for optoelectronic enhancement of ultrathin Cu(In,Ga)Se<sub>2</sub> solar cells. *ACS Appl Mater Interfaces*. 2016;8(46):31646-31652.
15. Bose S, Cunha JMV, Suresh S, et al. Optical lithography patterning of SiO<sub>2</sub> layers for interface passivation of thin film solar cells. *Sol RRL*. 2018;2(12):180021216.
16. Ezaei NAR, Sabella OLI, Roon ZEV, Zeman M. Quenching Mo optical losses in CIGS solar cells by a point contacted dual-layer dielectric spacer: a 3-D optical study. *Opt Exp Dermatol*. 2018;26(2):39-53.
17. Cunha J, Oliveira K, Lontchi J, Lopes TS, Salomé PMP. High-performance and industrially viable nanostructured SiO<sub>x</sub> layers for interface passivation in thin film solar cells. *Solar RRL*. 2021;5(3):2000534.
18. Lontchi J, Zhukova M, Kovacic M, et al. Optimization of back contact grid size in Al<sub>2</sub>O<sub>3</sub>-rear-passivated ultrathin CIGS PV cells by 2-D simulations. *IEEE J Photovoltaics*. 2020;10(6):1908-1917.
19. Nakada T, Hirabayashi Y, Tokado T, Ohmori D, Mise T. Novel device structure for Cu(In,Ga)Se<sub>2</sub> thin film solar cells using transparent conducting oxide back and front contacts. *Sol. Energy*. 2004;77(6):739-747.
20. Heinemann MD, Efimova V, Klenk R, et al. Cu(In,Ga)Se<sub>2</sub> superstrate solar cells: prospects and limitations. *Prog. Photovolt. Res. Appl.* 2015;23(10):1228-1237.
21. Saifullah M, Kim D, Cho J-S, et al. The role of NaF post-deposition treatment on the photovoltaic characteristics of semitransparent ultrathin Cu(In,Ga)Se<sub>2</sub> solar cells prepared on indium-tin-oxide back contacts: a comparative study. *J Mater Chem A*. 2019;7(38):21843-21853.
22. Li Y, Yin G, Gao Y, Köhler T, Lucaßen J, Schmid M. Sodium control in ultrathin Cu(In,Ga)Se<sub>2</sub> solar cells on transparent back contact for efficiencies beyond 12%. *Sol. Energy Mater. Sol. Cells*. 2021;223:110969.
23. Yin G, Manley P, Schmid M. Light trapping in ultrathin CuIn<sub>1-x</sub>Ga<sub>x</sub>Se<sub>2</sub> solar cells by dielectric nanoparticles. *Sol Energy*. 2018;163:443-452.
24. Yin G, Knight MW, van Lare M-C, Solà Garcia MM, Polman A, Schmid M. Optoelectronic Enhancement of Ultrathin CuIn<sub>1-x</sub>Ga<sub>x</sub>Se<sub>2</sub> Solar Cells by Nanophotonic Contacts. *Adv Opt Mater*. 2017;5(5):1600637.
25. Schneider T, Tröndle J, Fuhrmann B, Syrowatka F, Sprafke A, Scheer R. Ultrathin CIGSe Solar Cells with Integrated Structured Back Reflector. *Sol RRL*. 2020;4(10):2000295.
26. Louis G, Andrea C, Chao CW, et al. Interface engineering of ultrathin Cu(In,Ga)Se<sub>2</sub> solar cells on reflective back contacts. *Prog Photovolt Res Appl*. 2020;29:212-221.
27. Gouillart L, Chen W-C, Cattoni A, et al. Reflective back contacts for ultrathin Cu(In,Ga)Se<sub>2</sub>-based solar cells. *IEEE J. Photovoltaics*. 2020;10:250-254.
28. Schmid M, Caballero R, Klenk R, et al. Experimental verification of optically optimized CuGaSe<sub>2</sub> top cell for improving chalcopyrite tandems. *EPJ Photovoltaics*. 2010;1:10601.
29. Young DL, Abushama J, Noufi R, Li X, Coutts TJ, A new thin-film CuGaSe/sub 2//Cu (In, Ga) Se/sub 2/bifacial, tandem solar cell with both junctions formed simultaneously in IEEE Conference on Photovoltaic Specialists, IEEE, 2002, pp. 608-611.
30. Kim D, Shin SS, Lee SM, et al. Flexible and semi-transparent ultra-thin CIGSe solar cells prepared on ultra-thin glass substrate: a key to flexible bifacial photovoltaic applications. *Adv Funct Mater*. 2020;30(36):2001775.
31. Simchi H, Larsen JK, Kim K, Shafarman W. Improved performance of ultrathin Cu(In,Ga)Se<sub>2</sub> solar cells with a backwall superstrate configuration. *IEEE J. Photovoltaics*. 2014;4(6):1630-1635.
32. Larsen JK, Simchi H, Xin P, Kim K, Shafarman WN. Backwall superstrate configuration for ultrathin Cu(In,Ga)Se<sub>2</sub> solar cells. *Appl Phys Lett*. 2014;104(3):033901.
33. Simchi H, McCandless BE, Meng T, Shafarman WN. Structure and interface chemistry of MoO<sub>3</sub> back contacts in Cu(In,Ga)Se<sub>2</sub> thin film solar cells. *J Appl Phys*. 2014;115(3):033514.
34. Saifullah M, Kim K, Shahzad R, Gwak J, Park JH. Insertion of the AGS layer at the CIGSe/ITO interface: A way to reduce the formation of the GaOx interfacial phase in CIGSe solar cells. *Sol. Energy Mater. Sol. Cells*. 2018;178:29-37.
35. Saifullah M, Rasool S, Ahn S, et al. *ACS Appl. Mater Interfaces*. 2018;11(1):655-665.
36. Son YS, Yu H, Park JK, Kim WM, Jeong J. Control of structural and electrical properties of indium tin oxide (ITO)/Cu(In,Ga)Se<sub>2</sub> interface for transparent back-contact applications. *J Phys Chem C*. 2019;123:1635-1644.
37. Eisenbarth T, Caballero R, Nichterwitz M, Kaufmann CA, Unold T. Characterization of metastabilities in Cu(In,Ga)Se<sub>2</sub> thin-film solar cells by capacitance and current-voltage spectroscopy. *J Appl Phys*. 2011;110(9):094506.
38. Mollica F, Jubault M, Donsanti F, et al. Light absorption enhancement in ultra-thin Cu(In,Ga)Se<sub>2</sub> solar cells by substituting the back-contact with a transparent conducting oxide based reflector. *Thin Solid Films*. 2017;633:202-207.
39. Chantana J, Arai H, Minemoto T. Trap-assisted recombination for ohmic-like contact at p-type Cu(In,Ga)Se<sub>2</sub>/back n-type TCO interface in superstrate-type solar cell. *J Appl Phys*. 2016;120(4):045302.
40. Burgelman M, Nollet P, Degraeve S. Modelling polycrystalline semiconductor solar cells. *Thin Solid Films*. 2000;361:527-532.
41. Klenk R. Characterisation and modelling of chalcopyrite solar cells. *Thin Solid Films*. 2001;387(1-2):135-140.
42. Villanueva-Tovar A, Kodalle T, Kaufmann CA, Schlattmann R, Klenk R. Limitation of current transport across the heterojunction in Cu(In,Ga)Se<sub>2</sub> solar cells prepared with alkali fluoride postdeposition treatment. *Solar RRL*. 2020;4(4):1900560.
43. Yin G, Song M, Schmid M. Rear point contact structures for performance enhancement of semi-transparent ultrathin Cu(In,Ga)Se<sub>2</sub> solar cells. *Sol Energy Mater sol Cells*. 2019;195:318-322.
44. Scheer R & Schock HW. *Chalcogenide photovoltaics*, 2011, ISBN: 978-3-527-31459-1, P77.
45. Ott T, Schonberger F, Walter T, et al. Verification of phototransistor model for Cu(In,Ga)Se<sub>2</sub> solar cells. *Thin Solid Films*. 2015;582:392-396.

## SUPPORTING INFORMATION

Additional supporting information may be found in the online version of the article at the publisher's website.

**How to cite this article:** Tu Y, Li Y, Klenk R, Yin G, Schmid M. Is a passivated back contact always beneficial for Cu (In,Ga) Se<sub>2</sub> solar cells? *Prog Photovolt Res Appl*. 2022;30(4):393-400. doi:10.1002/pip.3500